IEEE Access
Multidisciplinary | Rapid Review | Open Access Journal

Received June 23, 2019, accepted July 13, 2019, date of publication July 18, 2019, date of current version August 5, 2019.

*Digital Object Identifier 10.1109/ACCESS.2019.2929615*

# Adaptive CDSC-Based Open-Loop Synchronization Technique for Dynamic Response Enhancement of Active Power Filters

**YACINE TERRICHE[1], MUHAMMAD UMAIR MUTARRAF[1], MOJTABA MEHRZADI[1], ABDEREZAK LASHAB[1], JOSEP M. GUERRERO[1], (Fellow, IEEE), JUAN C. VASQUEZ[1], (Senior Member, IEEE), AND DJALLEL KERDOUN[2]**

[1]Energy Technology, Aalborg University, 9220 Aalborg, Denmark
[2]Department of Electrical Engineering, University of Frères Mentouri Constantine 1, Constantine 25001, Algeria

Corresponding author: Yacine Terriche (yte@et.aau.dk)

**ABSTRACT** The shunt active power filters (SAPFs) are broadly utilized to improve the power quality (PQ) issues of electric power systems. A crucial issue in implementing these filters is the accurate estimation of the grid voltage phase/frequency. Indeed, the dynamic behavior and the performance of the SAPF strongly rely on this point. To deal with this challenge, a fast yet effective open-loop synchronization (OLS) technique based on Cascaded Delayed Signal Cancellation (CDSC) is presented in this paper. The proposed technique can reject the odd-order harmonics, the DC offset of the grid voltage, and its dynamic response during transients take an only half cycle of the fundamental frequency. To adapt the proposed OLS technique to the frequency changes, an efficient frequency estimator is also presented. The effectiveness of the proposed OLS technique is demonstrated using simulation and experimental results.

**INDEX TERMS** Cascaded delayed signal cancellation (CDSC) operators, open loop synchronization (OLS) technique, phase and frequency estimators, shunt active power filter.

## I. INTRODUCTION

In recent years, the use of power electronic converters (PECs) on the level of terrestrial grids or/and micro-grids have been growing immensely [1]. Indeed, these devices offer several advantages such as high efficiency, economical size, high reliability, fast dynamic response, etc. These converters, however, are often highly nonlinear and, therefore, cause large harmonics in power systems. [2]. The classical solution to mitigate this problem is the application of passive power filters (PPFs) [3], [4]. The PPFs can mitigate the most dominant harmonics, and compensate for a degree of reactive power. However, their application tends to worsen under frequency drifts. Moreover, problems such as the risk of resonance, fixed tuning, heavyweight and large size limit their application. In the last decade, the SAPFs appeared as an alternative to overcome the shortcomings of the PPFs [5], [6]. In addition to harmonics suppression, the SAPFs have the ability to compensate for the power factor (PF) and imbalance [6]. An essential part of implementing the SAPFs is the algorithm of determining the reference compensating current (RCC). This algorithm, which highly affects the SAPF performance, can be implemented in different ways. The available approaches can be broadly classified into time-domain and frequency domain approaches. [7]. The time domain techniques such as the synchronous reference frame method (SRF) are characterized by their simplicity and ease of implementation [8]. Fig. 1 presents a SAPF based on the SRF method for RCCs extraction. Based on linear low-pass filters, the SRF technique can easily separate between the harmonic perturbations and the positive sequence of the fundamental. Moreover, the SRF method can easily compensate for the PF by performing Park transformation using the phase angle of the voltage. Therefore, accurate information of the phase voltage is a crucial part to be detected inside the RCC algorithm. Several types of synchronization techniques have been proposed in the literature. Using an SRF phase-locked loop (hereafter called SRF-PLL) is the most popular way for the synchronization of a grid-tied inverter [9]. The SRF-PLL is a non-linear closed-loop system that synchronizes the error between the input and output in phase and frequency [10]. The SRF-PLLs can provide good performance under nominal grid conditions. However, their performance tends to worsen when the grid undergoes severe conditions.

The associate editor coordinating the review of this manuscript and approving it for publication was Eklas Hossain.

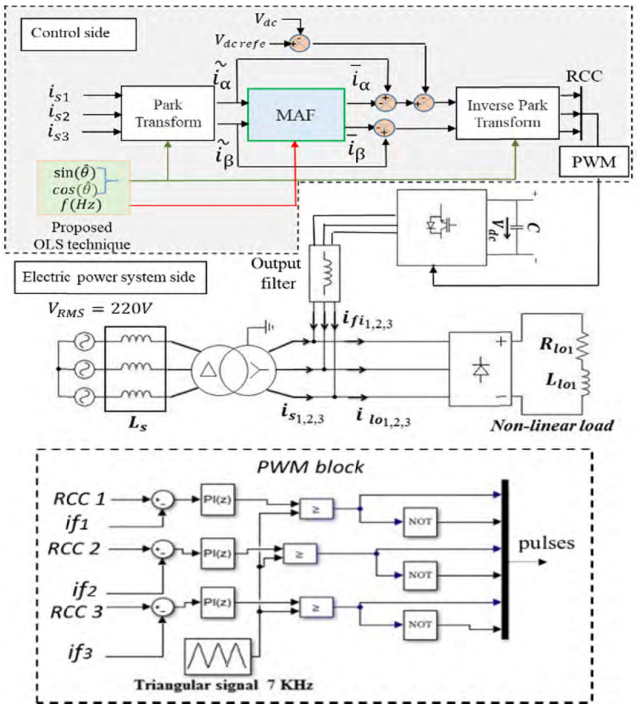


**FIGURE 1.** Schematic diagram of SAPF.

This problem might be mitigated by narrowing the bandwidth in the tuning procedure. This solution, however, would be at the expense of a slow response during transients [11]. In order to avoid this shortcoming, several types of filters have been integrated with the PLLs to enhance their disturbance rejection capabilities [9]. However, since the PLLs are featured by a negative feedback system, integrating harmonic filters with them results in slowing their dynamic response (usually more than two cycles). Other alternative synchronization techniques are based on the instantaneous symmetrical component theory [12]–[14]. Although some of these algorithms provide good dynamic behavior under nominal and off-nominal frequency, their harmonic rejection capability is insufficient.

Under severe grid contamination, the OLS techniques can perform sufficiently by integrating classical filters such as non-linear least-square solution [15], [16], discrete Fourier transform (DFT) [11], Kalman filter [17], and low-pass notch filter [18], and the moving average filter [19]. However, these filters contain a frequency-dependent behavior, which implies that their disturbance rejection capability degrades under frequency drifts. In order to overcome this limitation, a structure is proposed in [20] and [17], which adopt the filters with the estimated frequency. However, the series connection of the filter with the frequency estimator might result in instability issues due to the frequency feedback loop; therefore, this solution requires accurate stability analysis, which indicates that this technique is not strictly OLS technique [16]. In [11], [18] a second frequency estimator is employed separately from the phase estimator to adopt the filters. Hence, the OLS method keeps its characteristics and remains stable. However, adding extra frequency estimator leads to increase the computation burden and complexity. Furthermore, the calculation of the trigonometric functions (sine and cosine) are required in most techniques that are based on the open-loop synchronization [18]–[21]. An OLS technique based on $\alpha - \beta$ frame cascaded delayed signal cancellation ($\alpha - \beta$CDSC) based filter is proposed in [16]. The phase and frequency detectors are implemented separately, which makes the technique totally stable. Moreover, this technique does not need the calculation of the trigonometric functions, which is an advantage for cheap digital implementation devices. However, in the presence of odd-order harmonics and the DC offset, the transient response of this technique requires at least one cycle to reach the steady state.

In this paper, an OLS technique based on $\alpha - \beta$ frame cascaded delayed signal cancellation ($\alpha - \beta$CDSC) based filter is proposed to improve the dynamic response of SAPFs. In contradiction with the techniques proposed in [6], [11], [15]–[19], [21], [22], that require at least one cycle to give precise information of the phase in the existence of the odd harmonics and the dc component, the proposed technique can achieve that in solely a half cycle. Furthermore, the traditional way of estimating the grid frequency after the filtering process is available in [17], [23]. However, this method causes a detection error, mainly when decreasing the sampling frequency. An enhanced estimator, which can correct the error at low sampling frequency is proposed in [16]. Although this estimator can provide accurate estimation under grid frequency variations, it requires a window width of one and a half cycle which is a bit long. In this paper, an efficient and self-dependent frequency estimator is proposed. This estimator provides accurate frequency tracking with faster transient to adapt the proposed OLS technique to give precise phase estimation under severe grid conditions. The even harmonics are disregarded in this paper due to their insignificant values in most applications.

The rest of the paper is organized as follows: Section II provides an overview of the OLS technique based on the moving average filter (MAF) and $\alpha - \beta$CDSC based filter. Section III presents the proposed phase/frequency estimators. Section IV addresses the simulation results. Section V conducts the experimental validation. And Section VI concludes this paper.

## II. OVERVIEW OF OLS TECHNIQUE BASED ON MAF AND $\alpha - \beta$CDSC

The grid voltage of a three-phase power system can be expressed in both rotating space vector and time domain respectively as:

$$\vec{V}_{s1,2,3} = \frac{2}{3}(V_{s1} + aV_{s2} + a^2V_{s3}) \quad (1)$$

$$V_{s1,2,3}(t) = V_{\max}\cos(wt + k\frac{2\pi}{3}) \quad (2)$$

where $a$ is a unit-length rotating factor and expressed as: $a = e^{j\frac{2\pi}{3}} = -1/2 + j\sqrt{3}/2$, and $k$ is set to $0, -1$ and 1 for three

phases of the system. The coordination of the grid voltage in the stationary reference frame can be attained as:

$$\begin{bmatrix} \vec{V}_\alpha \\ \vec{V}_\beta \end{bmatrix} = \frac{2}{3}\begin{bmatrix} 1 & -\frac{1}{2} & -\frac{1}{2} \\ 0 & \sqrt{\frac{3}{2}} & -\sqrt{\frac{3}{2}} \end{bmatrix} \cdot \begin{bmatrix} \vec{V}_{s1} \\ \vec{V}_{s2} \\ \vec{V}_{s3} \end{bmatrix} = V_\alpha + jV_\beta \quad (3)$$

Note that in (3) $V_\alpha$ can represent the real part of the coordination, while $V_\beta$ is the imaginary part, which implies that the shift between them is $\pi/2$. Based on the fundamental theorem of algebra, the magnitude and the instantaneous phase of the grid voltage can respectively be expressed as:

$$V_{s\max} = \sqrt{V_\alpha(t)^2 + V_\beta(t)^2} \quad (4)$$

$$\hat{\theta} = \arctan(\frac{V_\beta(t)}{V_\alpha(t)}) \quad (5)$$

Since the grid voltage until now is considered balanced and free of harmonics, then (5) can be simplified as:

$$\hat{\theta} = \arctan\left(\frac{V_{f\max}\sin(\omega t)}{V_{f\max}\cos(\omega t)}\right) = \arctan(\tan(\omega t)) = \omega t \quad (6)$$

After that, the frequency $\omega$ of the system can be estimated by deriving $\hat{\theta}$ as formulated in (7).

$$\frac{d\hat{\theta}}{dt} = d\omega t/dt = \omega \quad (7)$$

However, since in many applications the grid voltage can be harmonically contaminated and unbalanced, then it can be represented as:

$$\begin{aligned} \begin{bmatrix} \vec{V}_\alpha \\ \vec{V}_\beta \end{bmatrix} &= \sum_{h=-\infty}^{\infty} V_{\alpha h} + j\sum_{h=-\infty}^{\infty} V_{\beta h} \\ &= \sum_{h=-\infty}^{\infty} V_{\max h}\cos(h\omega t + \theta_h) \\ &\quad + j\sum_{h=-\infty}^{\infty} V_{\max h}\sin(h\omega t + \theta_h) \end{aligned} \quad (8)$$

where $hwt$ and $\theta_h$ denote respectively the instantaneous phase angle and the initial phase of each harmonic. $h$ can be in the following orders $\pm1, \pm2, \pm3, \ldots$ etc. The signs $+$ and $-$ indicate respectively the positive and negative sequences of each harmonic with regard to the fundamental component. Estimating the phase angle in the existence of the perturbation becomes more complex

$$\tilde{\theta} = \arctan\left(\frac{V_{f\max}\sin(\omega t) + \sum_{h=\pm2,\pm3\ldots}^{\pm\infty} V_{h\max}\sin(h\omega t + \theta_h)}{V_{f\max}\cos(\omega t) + \sum_{h=\pm2,\pm3\ldots}^{\pm\infty} V_{h\max}\cos(h\omega t + \theta_h)}\right) \quad (9)$$

It is noteworthy to observe that the phase of the fundamental signal obtained from (6) and (9) is an increasing repetitive signal in a right-angled triangle form. The incorporation of

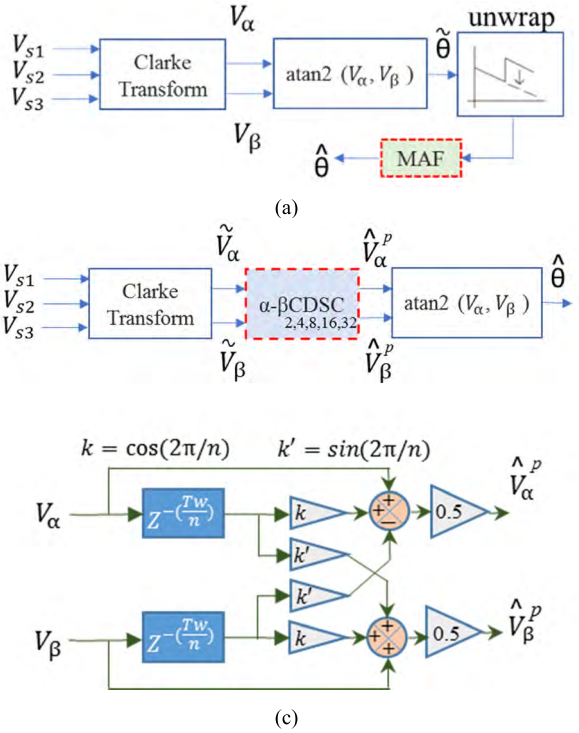


**FIGURE 2.** OLS technique. (a) OLS technique based on MAF. (b) OLS technique based on $\alpha - \beta$CDSC. (c) Discrete-time domain of one $\alpha - \beta$DSC operator.

the MAF (see Fig. 2 (a)) which acts as a linear filter, can reject the perturbation with a window width $T_w$ that corresponds to the type of perturbation (harmonic contamination, unbalance and dc offset). For a certain signal *A(t),* which can be voltage or current, the application of the MAF in continues and discrete domains can be expressed as:

$$Y(t) = \frac{1}{T_w}\int_{t-T_w}^{t} A(t)dt \quad (10)$$

$$Y(k) = \frac{1}{N}\sum_{n=0}^{N-1} Y(K-n) \quad (11)$$

Since the periodic signals are characterized by a repetition every certain cycle, the MAF is designed to estimate the mean value of the perturbation by storing a certain amount of data and subtracts it from its similar negative one. In order to facilitate the behavior of the MAF, the Laplace domain of the transfer function of the MAF is formulated as:

$$G_{MAF}(s) = \frac{1 - e^{-T_w s}}{T_w s} \quad (12)$$

The application of Padé approximation results in:

$$e^{-T_w s} \approx \frac{1 - (-T_w s/2)}{T_w s + (-T_w s/2)} \Rightarrow G_{MAF}(s) = \frac{1}{1 + (T_w s/2)} \quad (13)$$

It is noteworthy to observe that the transformation characteristic of the harmonics based on (7) has similar characteristics to the transformation from the $\alpha - \beta$ stationary frame to

$d-q$ rotating frame. Which implies that the fundamental positive sequence becomes a DC signal, while the odd harmonics of the order $h$jump to the order $h-1$. Therefore, for eliminating the harmonics of the order $6h \pm 1$ (such as three-phase diode rectifier harmonics: $-5^{\text{th}}, +7^{\text{th}}, -11^{\text{th}}, +13^{\text{th}}, \ldots$), $T_w$ can be selected to $T_w = 1/(6 \cdot f)$ which results in faster transient response. The existence of tripplen harmonics, however, requires a larger window width $T_w = 1/(2 \cdot f)$ to be rejected. While the existence of the dc-offset, which appears in (9) as a sinusoidal signal with a frequency, which corresponds, to the nominal one needs a window width of one cycle ($T_w = 1/f$). Although the application of the MAF is computationally effective, its implementation for the OLS techniques might require the unwrap block so as it can relate the output of each period with the next input as presented in [19]. Despite the fact that the unwrap block enables the MAF to work effectively, the unwrapped signal is continuously increasing to infinity. Hence, its application is not suitable for real applications due to the limit of digital signal processing and control cards. However, the incorporation of the MAF in the d-q synchronous frame does not require the unwrap block since the positive sequence of the fundamental is DC. Thereby, this paper invests the advantages of the MAF by incorporating it into the SRF algorithm to extract the RCC of the current, while the $\alpha - \beta$CDSC filter is dedicated to the voltage as depicted in Fig. 1.

The $\alpha - \beta$CDSC filter has similar behavior to the MAF in terms of harmonic rejection. Fig. 2 (b) shows the OLS technique, which is, based on $\alpha - \beta$CDSC operators, and Fig. 2 (c) presents the digital implementation of each operator. The transfer function of one operator of $\alpha - \beta$CDSC, which is depicted in Fig. 1 (c), is expressed as [24]–[26]:

$$\begin{bmatrix} \vec{V}_\alpha^{\,p} \\ \vec{V}_\beta^{\,p} \end{bmatrix} = \overbrace{\frac{1}{2}\left[1 + e^{\frac{j2\pi}{n}} e^{\frac{-Tw}{n}s}\right]}^{\alpha-\beta\text{DSC}} \begin{bmatrix} \vec{V}_\alpha \\ \vec{V}_\beta \end{bmatrix} \tag{14}$$

where the superscript $p$ denotes the positive sequence. $n$ is called the delayed factor, setting $n = 4$ results in rejecting the $-5^{\text{th}} + 7^{\text{th}}$ and the negative sequence component [24]. According to [24], in order to reject all the odd harmonics, four operators of $\alpha - \beta$DSC should be cascaded in series with different values of $n(n = 4, 8, 16, 32)$. Consequently, the transient response of the cascaded operators increases to around half cycle. On the other hand, the rejection of the dc offset requires an extra operator cascaded with the previous operators with $n = 2$, thus the transient response of the sum of the operators increases to around one cycle. Hence, (14) can be expressed as:

$$\begin{bmatrix} \vec{V}_\alpha^{\,p} \\ \vec{V}_\beta^{\,p} \end{bmatrix} = \prod_{n=2,4,8,16,32} \frac{1}{2}\left[1 + e^{\frac{j2\pi}{n}} e^{\frac{-Tw}{n}s}\right] \begin{bmatrix} \vec{V}_\alpha \\ \vec{V}_\beta \end{bmatrix} \tag{15}$$

Fig. 3 (a) depicts the Bode plot of the MAF. It is obvious that the MAF acts as an ideal low-pass filter, and thereby cancel all the harmonics which corresponds to the length of $T_w$.

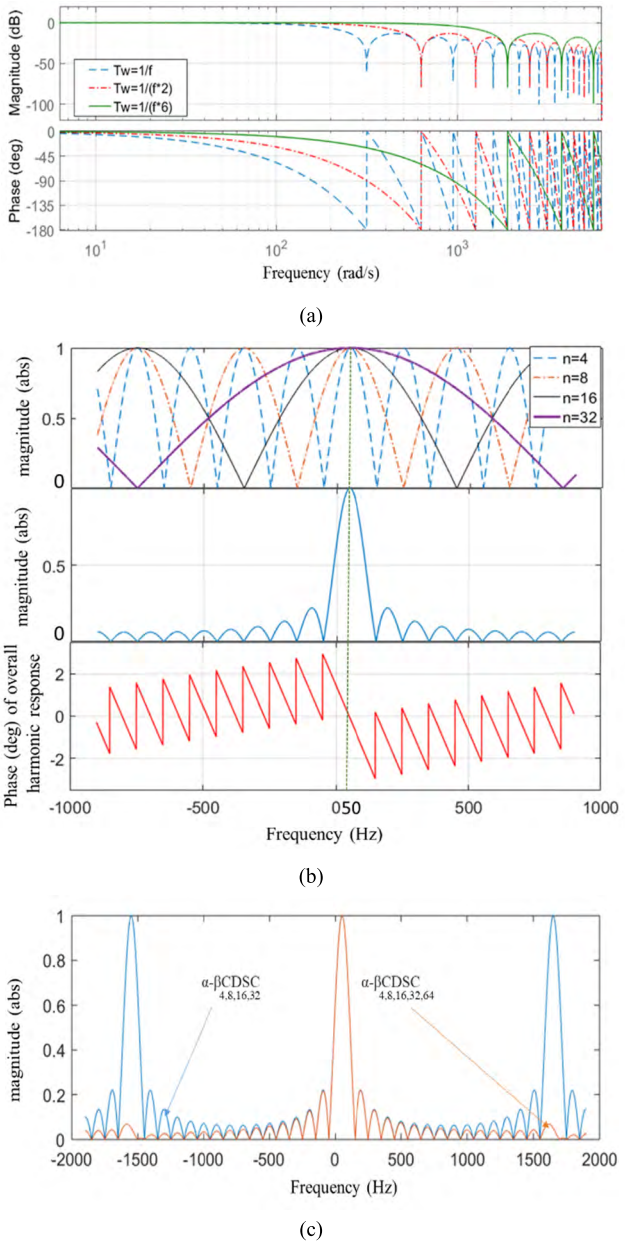


**FIGURE 3.** Bode plot of the MAF and the $\alpha - \beta$CDSC operator with different window width. (a) individual harmonic response of the MAF. (b) individual and overall harmonic response of the $\alpha - \beta$CDSC operator. (c) overall harmonic response of the $\alpha - \beta$CDSC operator with n = 4,8,16,32 and n = 4,8,16,32,64.

Fig. 3 (b) portrays the frequency response of $\alpha - \beta$CDSC. The first subplot shows the response of each operator with different values of $n(n = 4, 8, 16, 32)$, while the second and third subplots present respectively the overall response and phase of the cascaded operators. Based on Fig. (2), it can be observed that the MAF and the $\alpha - \beta$DSC have similar harmonic rejection behavior when the sum of the delays is half or one cycle. What distinguishes the $\alpha - \beta$CDSC operators is the implementation in the $\alpha - \beta$ stationary frame. Hence, its application does not require the unwrap block which enables

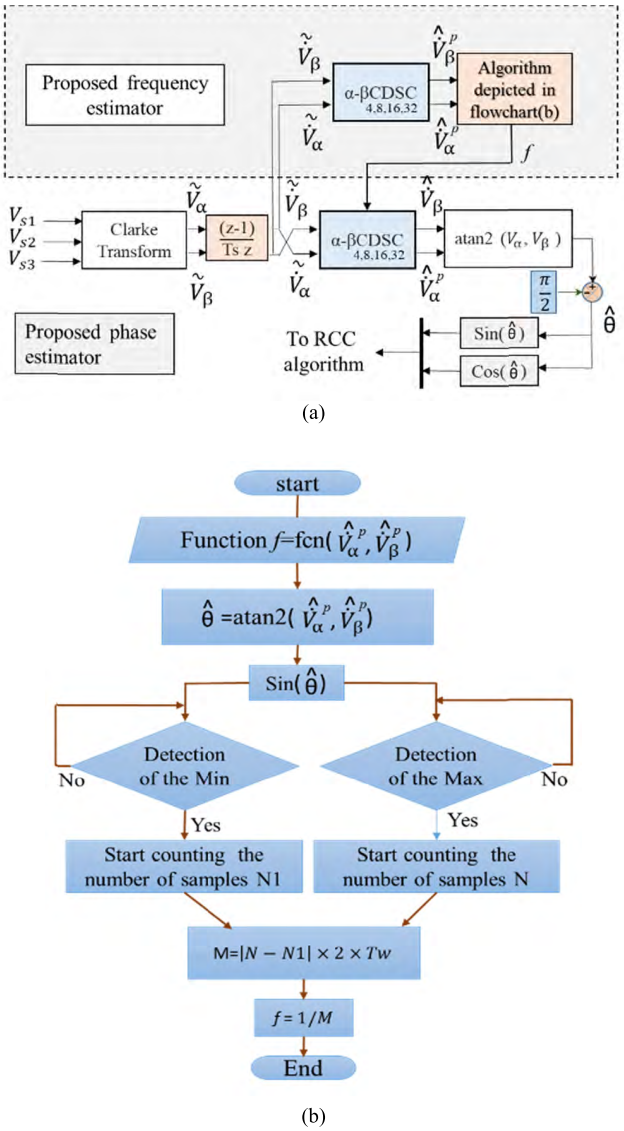


**FIGURE 4.** Proposed OLS technique. (a) Phase estimator. (b) Frequency estimator.

it to be applied in real applications based OLS techniques for grid phase/frequency estimation.

In case of applications where the signals are noisy (contaminated with high-order harmonics), adding an extra cascaded operator cascaded in series with the other operators with $n = 64$ results in enhancing the immunity of the $\alpha - \beta$CDSC filter in rejecting the high-order harmonics. In order to confirm this assertion, Fig. 3 (c) is presented. According, to Fig. 3 (c), it is clear that at some high order frequencies such as 1200 Hz, 1250 Hz, 1300 Hz…2200 Hz, where $n = 4, 8, 16, 32$ provide a poor harmonic rejection capability. However, in the case where $n = 4, 8, 16, 32, 64$, the rejection immunity of the $\alpha - \beta$CDSC filter is enhanced.

## III. PROPOSED OLS TECHNIQUE

From Fig. 3 it is obvious that the harmonic rejection capability of the $\alpha - \beta$CDSC operator and the MAF fails under frequency drifts, which results in phase shift and magnitude scaling of the fundamental positive sequence. Moreover, the existence of the DC offset requires an extra $\alpha - \beta$ CDSC with a delay factor of $n = 2$, which implies that the sum of the operators at $n = 2,4, 8, 16, 32$ causes a delay of approximately one cycle. To deal with these two shortcomings, the proposed OLS technique is designed so that the dc rejection capability with a negligible delay is achieved. Fig. 4 displays the proposed OLS technique, which is based on two estimators. These estimators are separated and connected in a parallel form. The first estimator is dedicated to estimating the grid frequency without any feedback system. Thus, it does not require any stability analysis or controller design. While the second estimator is dedicated to estimating the phase angle of the input signals and adapted by the proposed frequency estimator under frequency drifts. The main purpose of separating the estimators is to enhance the stability of estimating the frequency, which implies that if the phase estimator fails to provide an accurate estimation of the phase for certain reasons, the frequency estimator will not be affected by it.

In order to highlight the first contribution of the proposed technique, we assume that the grid voltage is affected by only the dc offset. Hence, the rotating phasor of the grid voltage can be expressed as shown in (16).

$$\begin{bmatrix} V^p_\alpha(t) \\ V^p_\beta(t) \end{bmatrix} = \begin{bmatrix} V_{dc\alpha} \\ V_{dc\beta} \end{bmatrix} + \begin{bmatrix} V^p_{\alpha 1} e^{j(\omega t + \theta^p_{\alpha 1})} \\ V^p_{\beta 1} e^{j(\omega t + \theta^p_{\beta 1})} \end{bmatrix} \tag{16}$$

By setting $s = jw$ and $T_w = 1/f$ in (16) and passing $V_\alpha(t)$ and $V_\beta(t)$ via $\alpha - \beta$DSC with $n = 2$ results in:

$$\begin{bmatrix} V^p_\alpha(t) \\ V^p_\beta(t) \end{bmatrix} = \begin{bmatrix} V_{dc\alpha} \\ V_{dc\beta} \end{bmatrix} + \begin{bmatrix} V^p_{\alpha 1} e^{j(\omega t + \theta^p_{\alpha 1})} \\ V^p_{\beta 1} e^{j(\omega t + \theta^p_{\beta 1})} \end{bmatrix} \frac{1}{2} \left[ 1 + e^{\frac{j2\pi(1 - Tw \cdot f)}{n}} \right] \tag{17}$$

After some mathematical manipulations, (17) becomes:

$$\begin{bmatrix} \hat{V}^p_\alpha(t) \\ \hat{V}^p_\beta(t) \end{bmatrix} = \begin{bmatrix} V^p_{\alpha 1} e^{j(\omega t + \theta^p_{\alpha 1})} \\ V^p_{\beta 1} e^{j(\omega t + \theta^p_{\beta 1})} \end{bmatrix} \tag{18}$$

where $\hat{}$ denotes the filtered signals. From (18), one can conclude that the dc offset requires a delay of $n = 2$ to be rejected. However, according to Fig. 4 (a), the proposed technique can reject the dc offset by inserting a derivative before the operators $\alpha - \beta\text{CDSC}_{4,8,16,32}$ as formulated in (19), and thereby there is no time delay caused during the rejection of the DC offset. Therefore, the proposed technique always benefits from a half cycle faster transient response comparing to the previous methods.

$$\begin{aligned} \frac{d}{dt} \begin{bmatrix} V^p_\alpha(t) \\ V^p_\beta(t) \end{bmatrix} &= \frac{d}{dt} \left( \begin{bmatrix} V_{dc\alpha} \\ V_{dc\beta} \end{bmatrix} + \begin{bmatrix} V^p_{\alpha 1} e^{j(\omega t + \theta^p_{\alpha 1})} \\ V^p_{\beta 1} e^{j(\omega t + \theta^p_{\beta 1})} \end{bmatrix} \right) \\ &= wj \begin{bmatrix} V^p_{\alpha 1} e^{j(\omega t + \theta^p_{\alpha 1})} \\ V^p_{\beta 1} e^{j(\omega t + \theta^p_{\beta 1})} \end{bmatrix} \end{aligned} \tag{19}$$

The derivative can amplify the high order harmonics. However, as it will be demonstrated in the results, the $\alpha-\beta$CDSC$_{4,8,16,32}$ offers high rejection capability even under small frequency drifts. From (19), one can observe that the results are similar to ones of (18), but without any time delay. The component $\omega$ in (19) is canceled in the process of extracting $\theta$ as shown in (6). While the shift $j$, which is resulted from the derivation process in the phase is compensated by adding $\frac{-\pi}{2}$ to $\hat{\theta}$ as depicted in Fig. 4 (a).

$$\hat{\theta} = \arctan\left(\frac{\hat{V_\beta}(t)}{\hat{V_\alpha}(t)}\right) - \frac{\pi}{2} \tag{20}$$

According to (17), if the grid frequency is at its nominal value, the term $Tw \cdot f$ will be equal to 1 for the positive sequence of the fundamental frequency of the voltages. However, when the grid undergoes some fluctuations, the term $Tw \cdot f$ is not equal to 1 anymore. Consequently, the accuracy of the $\alpha-\beta$CDSC tends to worsen. The traditional method for estimating the grid frequency is based on deriving the estimated phase [17], [23]. However, such techniques show low performance, mainly in applications where the sampling frequency is low. A simple yet effective estimator based on $\alpha-\beta$CDSC is proposed in [16] to compensate for the error caused by the traditional solutions. Although this estimator has offered improved results, it will be demonstrated in this paper that its accuracy degrades under severe grid conditions. Moreover, this estimator requires extra filtering block based on MAF, which slows down its response. With regard to avoiding this weakness, an efficient frequency estimator with a simple structure for grid-connected applications is proposed in this paper. As depicted in Fig. 4 (a), the procedures start by transforming the grid voltage from the $a-b-c$ stationary frame into the $\alpha-\beta$ stationary frame, then, inserting a derivative to reject the dc offset with zero time delay similar to the procedure of estimating the phase. After that, the operators $\alpha-\beta$CDSC$_{4,8,16,32}$ are applied in series to cancel the harmonic components. Next, the proposed algorithm, which is depicted in Fig. 3 (b) is applied to extract the frequency of the filtered signal. As will be demonstrated in Fig. 5 in the results section, the affection of frequency drifts does not much deteriorate the filtered stationary frame signal as it does with the dc signal that is extracted by the derivation of the arctangent. Therefore, the proposed technique extracts the sinus of the estimated $\theta$, then accurately detect the maximum and the minimum of the extracted signal. After that, it counts the number of samples $N$ and $N_1$ between the maximum and the minimum points for each half cycle. Finally, the frequency is estimated from the number of samples that are presented in (21).

$$f = \frac{1}{|N - N_1| \cdot 2 \cdot Tw} \tag{21}$$

## IV. SIMULATION RESULTS

The simulation results are carried out under the MATLAB/Simulink environment. For the sake of diversity and consistency, the simulation section focuses on the performance of the proposed technique in estimating the phase/frequency of a contaminated grid, while the experimental part examines the behavior of the proposed technique in enhancing the SAPF dynamic performance.

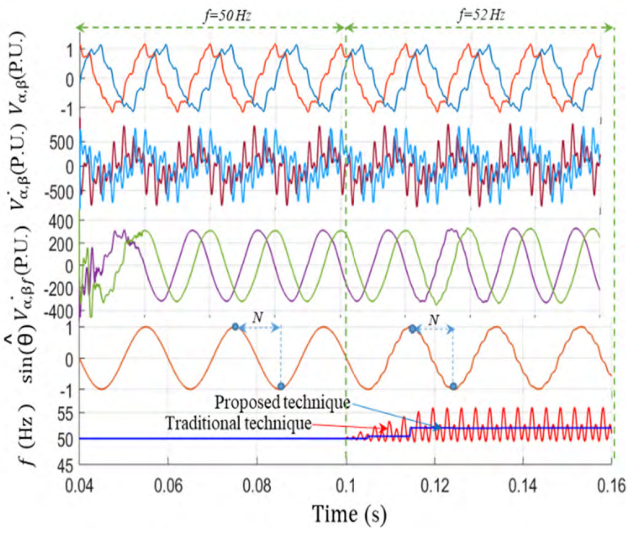


**FIGURE 5.** Performance of the proposed frequency estimator under frequency drifts and in the presence of harmonics.

Fig. 5 explains how the proposed frequency estimator can work effectively under frequency drifts and in the presence of harmonics. The first and second subplots present respectively a distorted signal and its derivative, while the third subplot portrays the filtered signal using $\alpha-\beta$CDSC$_{4,8,16,32}$ operators. It is obvious that under a frequency drift of 4% (50 Hz to 52 Hz), the quality of the filtered signal is a bit affected. Therefore, extracting the frequency using the aforementioned techniques results in some fluctuations that are shown in the last subplot with the red color. However, the distance between the maximum and minimum points of the sinusoidal filtered signal of the sinus block based on $\alpha-\beta$CDSC$_{4,8,16,32}$ are not affected by those harmonics; therefore, the proposed frequency estimator algorithm which is depicted in Fig. 4(b) can accurately extract the frequency as proved in the last subplot of Fig. 4 with the blue color.

Fig. 6 presents the behavior of the proposed OLS technique in estimating the frequency and phase of the grid voltage under frequency drift, phase jump, and voltage sag. The grid voltage, which is transformed to the stationary Alpha-Beta frame ($V_{\alpha,\beta}$), is contaminated with the odd harmonics and dc offset of respectively 10% and 20% of the voltage amplitude for the first phase the third phase. It is clear that the transient response of the proposed technique at the starting stage is faster (it takes only 0.01s to reach steady state) than the enhanced true open loop synchronization technique (ETOLS) which is proposed in [16]) (it takes about 0.028s to reach the steady state).

Moreover, in the instance 0.061s, a frequency drift of 4% is applied (the frequency changed from 50 Hz to 52 Hz). It is obvious that the proposed frequency estimator comprises a

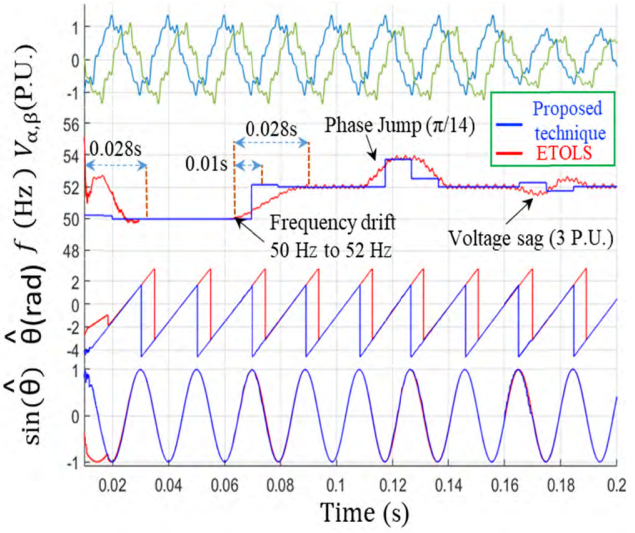


**FIGURE 6.** Performance of the proposed OLS technique in estimating the phase and frequency of the grid voltage under frequency drift, phase jump, and voltage sag.

**TABLE 1.** Experimental parameters.

| Devices | Parameters | Values |
|---|---|---|
| Power supply | Fundamental Voltages (RMS) : | $V_s = 230$ V |
| | -5th harmonic: | $V_{-5} = 30$ V |
| | 7th harmonic: | $V_7 = 20$ V |
| | -11th harmonic: | $V_{-11} = 10$ V |
| | 13th harmonic: | $V_{13} = 5$ V |
| | Main impedance | $L_s = 0.007$ *mH*, $R_s = 0.7\ \Omega$ |
| | Dc offset | $V_{s1,2,3} = +50$ V |
| | Unbalance | $V_{s1,3} = 230$ V, $V_{s2} = 180$ V |
| SAPF | dc link voltage | $V_{dc} = 650$ V |
| | dc link capacitor: | $C = 2200\ \mu F$ |
| | output filters: | $L_f = 15$ *mH*, $R_f = 1.9\ \Omega$ |

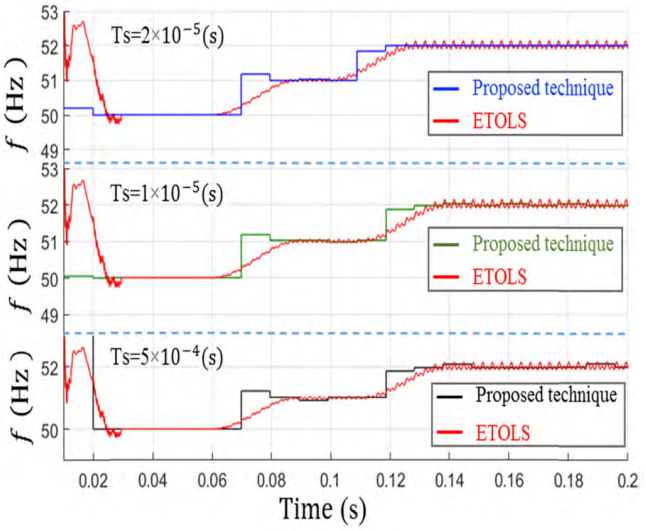


**FIGURE 7.** Performance of the proposed frequency estimator under different sampling time.

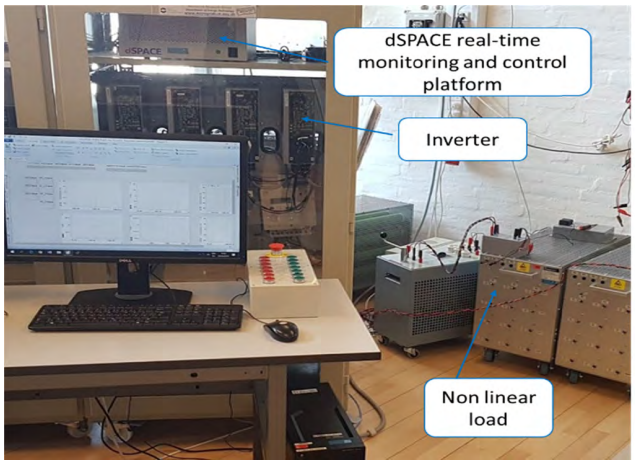


**FIGURE 8.** Experimental prototype of SAP.

faster behavior regarding the transient response (it needs only 0.01s to reach the steady state) comparing the one used in the ETOLS technique that requires about 0.028s, which is a bit long. Furthermore, in the instances 0.11s and 0.16s, a phase jump of ($\pi$/14) and a voltage sag of 0.3 p.u. have respectively occurred. It is observable that the proposed technique provides a faster and more accurate estimation with a transient response that lasts about a half cycle comparing to the ETOLS transient response that lasts almost a cycle and half. Note that the phase jump of $\pi$/14 causes a frequency overshoots for both techniques of about 2 Hz; however, the duration of the proposed technique is smaller than the one of the ETOLS. In addition, it is obvious that the estimator of the ETOLS causes some fluctuations under frequency changes, while the proposed technique keeps offering an accurate estimation. The subplots 3 and 4 of Fig. 5 present respectively the phase of the grid voltage and its sinus, which corresponds to the proposed, and the ETOLS techniques.

Fig. 7 shows the performance of the proposed frequency estimator under different sampling time $T_s$. It is observable that increasing the sampling time from 20 $\mu$s to 0.5 ms can slightly decrease the accuracy. However, this decrease is negligible compared with the fluctuations caused by the estimator of the ETOLS technique. Besides, the recent substantial development in digital signal processors such as dSPACE and FPGA cards enables the decrease of the sampling time, which enhances the accuracy of all advanced signal-processing algorithms.

## V. EXPERIMENTAL RESULTS

Fig. 8 portrays the experimental prototype of the developed SAPF which is depicted in Fig. 1. The MAF is implemented into the SRF to separate between the positive sequence of the fundamental current that appears as DC current in the rotating d-q frame and the harmonic components. The Park transformation is applied based on the phase angle extracted by the proposed OLS technique. While the MAF of the SRF

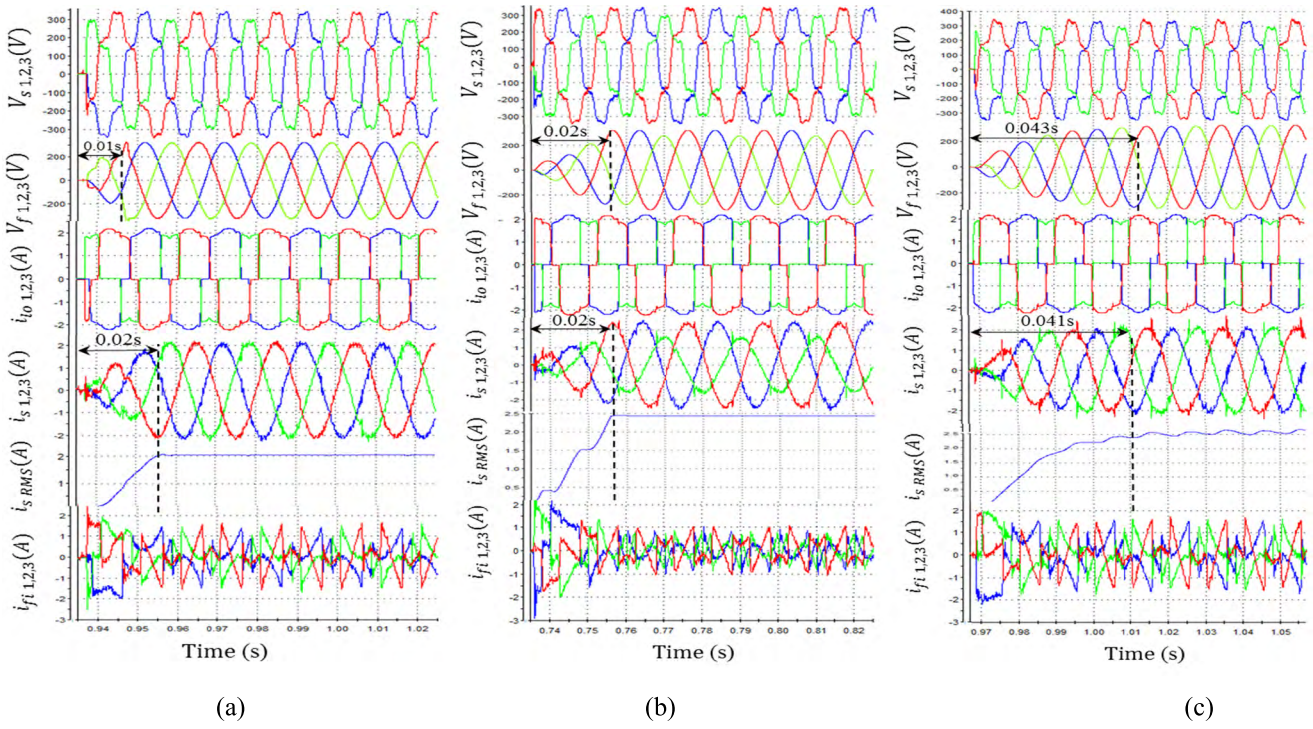


**FIGURE 9.** Experimental results of the dynamic response of SAPF under distorted and unbalanced voltage. (a) Proposed OLS technique. (b) DFT. (c) STF.

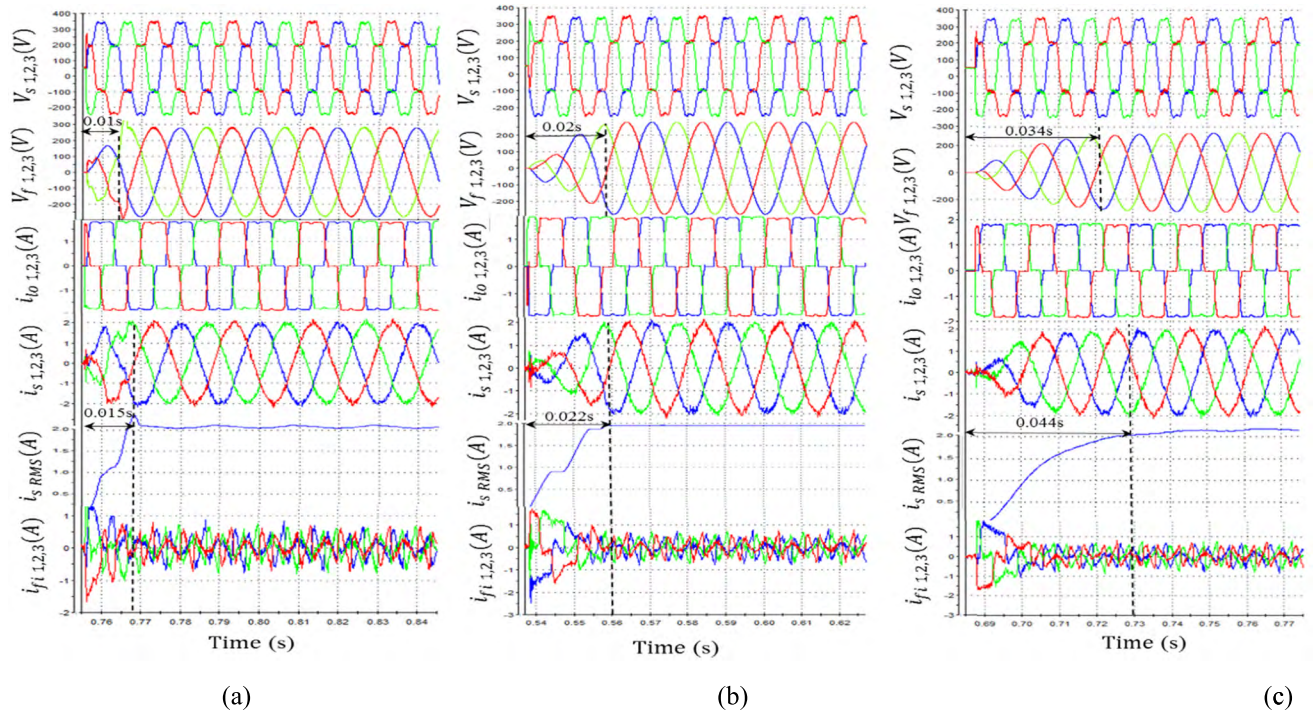


**FIGURE 10.** Experimental results of the dynamic response of SAPF under distorted voltage and DC offset. (a) Proposed OLS technique. (b) DFT. (c) STF.

can be adaptive under frequency drifts using the proposed frequency-based estimator. The RCC extracted by the SRF are fed to the PWM block to supply the pulses for the SAPF. The experimental setup consists of a three-phase source (Chroma, model 61845), a three-phase non-linear load, and a three-phase isolation transformer with leakage inductance. The proposed topology is implemented under MATLAB blocks with a digital signal processor (dSPACE-1006). The SAPF is implemented using two-level converter Danfoss 2.2. The voltages and currents are sensed using Hall effect sensors. The parameters of the experimental configuration are illustrated in table 1.

Fig. 9 presents the dynamic behavior of the SAPF under distorted and unbalanced voltage. For the sake of consistency, the proposed control method which is depicted in Fig. 4 is compared with two traditional techniques from the literature that are applied for APFs such as DFT [27], [28] and self-tuning filter (STF) [29]. The subplots of Fig. 9 represent respectively distorted voltage $V_s$, filtered load voltage $V_f$, load current $i_{lo}$, source current $i_s$, RMS value of source current $i_{sRMS}$ and load current $i_{fi}$. Extracting $V_f$ using the proposed technique is achieved by transforming the sinus and cosine of the estimated $\hat{\theta}$ into the $a-b-c$ stationary frame and multiplied with the voltage magnitude. It is very clear that $V_f$ extracted by the proposed technique provides faster dynamic response (0.01s) than DFT and STF, which they take respectively one cycle and more than two cycles to reach the steady state. Moreover, since the DFT is applied in $a-b-c$ stationary frame, it cannot reject the unbalance. Feeding the SRF algorithm with the phase $\hat{\theta}$ based on the proposed technique to perform Park transformation results in a faster transient response of $i_{sRMS}$ and $i_s$ with a total harmonic distortion (THD) less than 5%, which conform to IEC 61000-3-6 and IEEE 519-1992 standards. Although, $i_s$ filtered by the DFT takes also one cycle to reach the steady state, it cannot compensate for the unbalance. While the technique based on

## VI. CONCLUSION

This paper has proposed a fast yet effective OLS technique based on CDSC to enhance the dynamic response of the SAPF. The proposed technique has proved its efficacy in rejecting the odd harmonics and the DC offset of the grid voltage during estimating its phase angle in only a half cycle. In addition, in order to adopt the proposed OLS technique under frequency drifts, an efficient frequency estimator with a simple structure is proposed. Based on the obtained simulation results, it has been proved that the proposed OLS technique and the frequency estimator can accurately estimate the phase/frequency of the distorted voltage grid with fast transient response. Moreover, the proposed technique has been compared with traditional and advanced estimators to demonstrate its accuracy and faster response. The experimental results are presented to illustrate the dynamic response enhancement of the SAPF using the proposed technique and compared with traditional RCC techniques.

## REFERENCES


[1] A. Micallef, M. Apap, C. Spiteri-Staines, and J. M. Guerrero, "Mitigation of harmonics in grid-connected and islanded microgrids via virtual admittances and impedances," *IEEE Trans. Smart Grid*, vol. 8, no. 2, pp. 651–661, Mar. 2017.

[2] R. L. Smith and R. P. Stratford, "Power system harmonics effects from adjustable-speed drives," *IEEE Trans. Ind. Appl.*, vol. IA-20, no. 4, pp. 973–977, Jul. 1984.

[3] C. Kawann and A. E. Emanuel, "Passive shunt harmonic filters for low and medium voltage: A cost comparison study," *IEEE Trans. Power Syst.*, vol. 11, no. 4, pp. 1825–1831, Nov. 1996.

[4] Y. Terriche, D. Kerdoun, and H. Djeghloud, "A new passive compensation technique to economically improve the power quality of two identical single-phase feeders," in *Proc. IEEE 15th Int. Conf. Environ. Elect. Eng. (EEEIC)*, Jun. 2015, pp. 54–59.

[5] S. Bosch, J. Staiger, and H. Steinhart, "Predictive current control for an active power filter with LCL-filter," *IEEE Trans. Ind. Electron*, vol. 65, no. 6, pp. 4943–4952, Jun. 2018.

[6] Y. Terriche, S. Golestan, J. M. Guerrero, D. Kerdoune, and J. C. Vasquez, "Matrix pencil method-based reference current generation for shunt active power filters," *IET Power Electron.*, vol. 11, no. 4, pp. 772–780, Apr. 2018.

[7] A. M. Massoud, S. J. Finney, and B. W. Williams, "Review of harmonic current extraction techniques for an active power filter," in *Proc. 11th Int. Conf. Harmon. Qual. Power*, Sep. 2004, pp. 154–159.

[8] B. Singh and V. Verma, "Selective compensation of power-quality problems through active power filter by current decomposition," *IEEE Trans. Power Del.*, vol. 23, no. 2, pp. 792–799, Apr. 2008.

[9] S. Golestan, J. M. Guerrero, and J. C. Vasquez, "Three-phase PLLs: A review of recent advances," *IEEE Trans. Power Electron.*, vol. 32, no. 3, pp. 1894–1907, Mar. 2017.

[10] F. M. Gardner, *Phaselock Techniques*. Hoboken, NJ, USA: Wiley, 2005.

[11] F. Baradarani, M. R. Dadash Zadeh, and M. A. Zamani, "A phase-angle estimation method for synchronization of grid-connected power-electronic converters," *IEEE Trans. Power Del.*, vol. 30, no. 2, pp. 827–835, Apr. 2015.

[12] M. Karimi-Ghartemani and M. R. Iravani, "A method for synchronization of power electronic converters in polluted and variable-frequency environments," *IEEE Trans. Power Syst.*, vol. 19, no. 3, pp. 1263–1270, Aug. 2004.

[13] P. Rodriguez, A. Luna, M. Ciobotaru, R. Teodorescu, and F. Blaabjerg, "Advanced grid synchronization system for power converters under unbalanced and distorted operating conditions," in *Proc. 32nd Annu. Conf. IEEE Ind. Electron. (IECON)*, Nov. 2006, pp. 5173–5178.

[14] S. Alepuz, S. Busquets-Monge, J. Bordonau, J. A. Martinez-Velasco, C. A. Silva, J. Pontt, and J. Rodriguez, "Control strategies based on symmetrical components for grid-connected converters under voltage dips," *IEEE Trans. Ind. Electron.*, vol. 56, no. 6, pp. 2162–2173, Jun. 2009.

[15] Y. Terriche, J. M. Guerrero, and J. C. Vasquez, "Performance improvement of shunt active power filter based on non-linear least-square approach," *Electr. Power Syst. Res.*, vol. 160, pp. 44–55, Jul. 2018.

[16] S. Golestan, A. Vidal, A. G. Yepes, J. M. Guerrero, J. C. Vasquez, and J. Doval-Gandoy, "A true open-loop synchronization technique," *IEEE Trans. Ind. Informat.*, vol. 12, no. 3, pp. 1093–1103, Jun. 2016.

[17] A. Bagheri, M. Mardaneh, A. Rajaei, and A. Rahideh, "Detection of grid voltage fundamental and harmonic components using Kalman filter and generalized averaging method," *IEEE Trans. Power Electron.*, vol. 31, no. 2, pp. 1064–1073, Feb. 2016.

[18] K.-J. Lee, J.-P. Lee, D. Shin, D.-W. Yoo, and H.-J. Kim, "A novel grid synchronization PLL method based on adaptive low-pass notch filter for grid-connected PCS," *IEEE Trans. Ind. Electron.*, vol. 61, no. 1, pp. 292–301, Jan. 2014.

[19] E. Robles, J. Pou, S. Ceballos, J. Zaragoza, J. L. Martin, and P. Ibañez, "Frequency-adaptive stationary-reference-frame grid voltage sequence detector for distributed generation systems," *IEEE Trans. Ind. Electron.*, vol. 58, no. 9, pp. 4275–4287, Sep. 2011.

[20] C. J. Ramos, A. P. Martins, and A. S. Carvalho, "Frequency and phase-angle estimation using ordinary least squares," *IEEE Trans. Ind. Electron.*, vol. 62, no. 9, pp. 5677–5688, Sep. 2015.

[21] F. D. Freijedo, J. Doval-Gandoy, Ó. López, and E. Acha, "A generic open-loop algorithm for three-phase grid voltage/current synchronization with particular reference to phase, frequency, and amplitude estimation," *IEEE Trans. Power Electron.*, vol. 24, no. 1, pp. 94–107, Jan. 2009.

[22] S. Golestan, M. Ramezani, J. M. Guerrero, and M. Monfared, "Dq-frame cascaded delayed signal cancellation- based PLL: Analysis, design, and comparison with moving average filter-based PLL," *IEEE Trans. Power Electron.*, vol. 30, no. 3, pp. 1618–1632, Mar. 2015.

[23] C. A. Busada, H. G. Chiacchiarini, and J. C. Balda, "Synthesis of sinusoidal waveform references synchronized with periodic signals," *IEEE Trans. Power Electron.*, vol. 23, no. 2, pp. 581–590, Mar. 2008.

[24] Y. F. Wang and Y. W. Li, "Grid synchronization PLL based on cascaded delayed signal cancellation," *IEEE Trans. Power Electron.*, vol. 26, no. 7, pp. 1987–1997, Jul. 2011.

[25] L. Asiminoaei, F. Blaabjerg, and S. Hansen, "Evaluation of harmonic detection methods for active power filter applications," in *Proc. 20th Annu. IEEE Appl. Power Electron. Conf. Expo. (APEC)*, vol. 1, Mar. 2005, pp. 635–641.

[26] S. Gude and C.-C. Chu, "Single-phase enhanced phase-locked loops based on multiple delayed signal cancellation filters for micro-grid applications," *IEEE Trans. Ind. Appl.*, to be published.

[27] S. Gude and C.-C. Chu, "Three-phase PLLs by using frequency adaptive multiple delayed signal cancellation prefilters under adverse grid conditions," *IEEE Trans. Ind. Appl.*, vol. 54, no. 4, pp. 3832–3844, Jul./Aug. 2018.
[28] G. H. Hostetter, "Recursive discrete Fourier transformation," *IEEE Trans. Acoust., Speech, Signal Process.*, vol. 28, no. 2, pp. 184–190, Apr. 1980.
[29] S. Biricik, S. Redif, Ö. C. Ozerdem, S. K. Khadem, and M. Basu, "Real-time control of shunt active power filter under distorted grid voltage and unbalanced load condition using self-tuning filter," *IET Power Electron.*, vol. 7, no. 7, pp. 1895–1905, Jul. 2014.

**YACINE TERRICHE** received the B.S. degree in electrical engineering from the University of Science and Technology, Consatantine, Algeria, in 2011, and the M.S. degree in electrical engineering from the University of Constantine 1, Constantine, in 2013. He is currently pursuing the Ph.D. degree with the Department of Energy Technology, Aalborg University, Denmark. His research interests include power electronics, modeling, control, signal processing, power quality issues, active and passive power filters, and shipboard microgrids.

**MUHAMMAD UMAIR MUTARRAF** received the B.Sc. degree in electrical engineering from the University of Engineering and Technology, Lahore, Pakistan, in 2013, and the M.Eng. degree in control theory and control engineering from Xidian University, China, in 2017. He is currently pursuing the Ph.D. degree with the Department of Energy Technology, Aalborg University, Denmark. His research interests include power electronics, modeling, control, and integration of energy storages in AC and DC shipboard microgrids.

**MOJTABA MEHRZADI** received the B.Sc. degree in electrical engineering from the Department of Engineering and Technology, University of IAU, Iran, in 2007, and the M.Sc. degree in control theory and control engineering from IAU, Iran, in 2012. He is currently pursuing the Ph.D. degree with the Department of Energy Technology, Aalborg University, Denmark. His research interest includes power management systems of hybrid dynamic positioning shipboard.

**ABDEREZAK LASHAB**, photograph and biography not available at the time of publication.

**JOSEP M. GUERRERO** (S'01–M'04–SM'08–F'15) received the B.S. degree in telecommunications engineering, the M.S. degree in electronics engineering, and the Ph.D. degree in power electronics from the Technical University of Catalonia, Barcelona, in 1997, 2000, and 2003, respectively.

Since 2011, he has been a Full Professor with the Department of Energy Technology, Aalborg University, Denmark, where he is responsible for the Microgrid Research Program (www.microgrids.et.aau.dk). Since 2014, he has been the Chair Professor with Shandong University. Since 2015, he has been a Distinguished Guest Professor with Hunan University. Since 2016, he has been a Visiting Professor Fellow with Aston University, U.K., and a Guest Professor with the Nanjing University of Posts and Telecommunications. Since 2019, he became a Villum Investigator. His research interests is oriented to different microgrid aspects, including power electronics, distributed energy-storage systems, hierarchical and cooperative control, energy management systems, smart metering, and the Internet of Things for AC/DC microgrid clusters and islanded minigrids; recently, specially focused on maritime microgrids for electrical ships, vessels, ferries, and seaports. He has published more than 500 journal papers in the fields of microgrids and renewable energy systems, which are cited more than 30 000 times. In 2015, he was elevated as an IEEE Fellow for his contributions on "distributed power systems and microgrids." He received the Best Paper Award of the IEEE TRANSACTIONS ON ENERGY CONVERSION (2014–2015), and the Best Paper Prize of the IEEE-PES, in 2015. Moreover, he received the Best Paper Award of the *Journal of Power Electronics*, in 2016. During five consecutive years, from 2014 to 2018, he was awarded by Clarivate Analytics (former Thomson Reuters) as the Highly Cited Researcher. He is an Associate Editor for a number of the IEEE TRANSACTIONS.

**JUAN C. VASQUEZ** (M'12–SM'14) received the B.S. degree in electronics engineering from the Autonomous University of Manizales, Manizales, Colombia, and the Ph.D. degree in automatic control, robotics, and computer vision from BarcelonaTech-UPC, Spain, in 2004 and 2009, respectively. He was with the Autonomous University of Manizales, working as a Teaching Assistant and the Technical University of Catalonia, as a Postdoctoral Assistant, in 2005 and 2008, respectively. In 2011, he was an Assistant Professor, and was an Associate Professor with the Department of Energy Technology, Aalborg University, Denmark, in 2014. In 2019, he became a Full Professor, and is currently the Vice Programme Leader of the Microgrids Research Program (see microgrids.et.aau.dk). He was a Visiting Scholar at the Center of Power Electronics Systems (CPES), Virginia Tech, and a Visiting Professor at Ritsumeikan University, Japan. His current research interests include operation, advanced hierarchical and cooperative control, optimization, and energy management applied to distributed generation in AC/DC Microgrids, maritime microgrids, advanced metering infrastructures, and the integration of the Internet of Things and Energy Internet into the SmartGrid. He is an Associate Editor of the *IET Power Electronics* and a Guest Editor of the IEEE TRANSACTIONS ON INDUSTRIAL INFORMATICS SPECIAL ISSUE ON ENERGY INTERNET. In 2017 and 2018, he was awarded as the Highly Cited Researcher by Thomson Reuters. In 2019, he was a recipient of the Young Investigator Award 2019. He has published more than 300 journal papers in the field of microgrids, which in total are cited more than 15000 times. He is currently a member of the IEC System Evaluation Group SEG4 on LVDC Distribution and Safety for the use in Developed and Developing Economies, the Renewable Energy Systems Technical Committee TC-RES in IEEE Industrial Electronics, PELS, IAS, and PES Societies.

**DJALLEL KERDOUN** received the B.Sc. and M.Sc. degrees in electrical drive and automation of industrial and technological complexes from the Technical University, Institute of Energy of Moscow, Russia, in 1995 and 1997, respectively, and the Ph.D. degree in electrical engineering from the Technical University, Institute of Energy of Moscow, Russia, in 2001, for his work on asynchronous electric drive of spherical drum-type mills with use of voltage regulator.

Since 2004, he has been with the Department of Electrical Engineering, The University of Constantine1, Constantine, Algeria, first as a Research Assistant, then as a Lecturer in power electronic systems, with the Power electronics, Machines, and Control Group. Recently, he has become the Head of the Department of the Electrical Engineering, The University of Constantine1, Constantine, Algeria. His research interests include solid state drives, power converters, electrical machines, and wind and photovoltaic power generation.